MATHEMATICAL BIOSCIENCES
AND ENGINEERING
Volume **2**, Number **2**, April **2005**

http://www.mbejournal.org/

pp. **289–315**

PARAMETER ESTIMATION IN A COUPLED SYSTEM OF NONLINEAR SIZE-STRUCTURED POPULATIONS

Azmy S. Ackleh

Department of Mathematics, University of Louisiana at Lafayette
Lafayette, Louisiana 70504-1010

H. T. Banks

Center for Research in Scientific Computation, North Carolina State University
Raleigh, North Carolina 27695-8205

Keng Deng

Department of Mathematics, University of Louisiana at Lafayette
Lafayette, Louisiana 70504-1010

Shuhua Hu

Department of Mathematics, University of Louisiana at Lafayette
Lafayette, Louisiana 70504-1010

(Communicated by Stephen Gourley)

Abstract. A least squares technique is developed for identifying unknown parameters in a coupled system of nonlinear size-structured populations. Convergence results for the parameter estimation technique are established. Ample numerical simulations and statistical evidence are provided to demonstrate the feasibility of this approach.

1. **Introduction.** A typical *direct problem* for structured populations is to use the knowledge of underlying mechanism at an individual level, such as growth, mortality and reproduction rates, to deduce the behavior at population level. This approach has been extensively studied for many kinds of models, including structured and nonstructured populations. In practice, however, our knowledge of the vital rates may be incomplete [40]. In fact, in many animal and plant populations the processes at the individual level are not accessible to direct observation [47]. For example, for nonlinear structured models, the dependence of reproduction and mortality rates on the total population is sometimes unknown [37]. Even for linear structured models, one may be unable to obtain the exact dependence of the vital rates on the age or size structure [40]. In these cases, one resorts to an *inverse problem* approach, using knowledge about the behavior at the population level (e.g, observations of total population numbers) to deduce the underlying mechanisms at the individual level.

2000 *Mathematics Subject Classification.* 92D25, 65M32, 35L60.
Key words and phrases. parameter estimation, coupled system of nonlinear size-structured populations, finite difference approximation, numerical simulation, standard deviation.

In recent years many researchers have focused their attention on developing methodologies for solving inverse problems governed by structured population models (e.g, [1]–[3], [12]–[17], [19]–[23], [25]–[34], [40]–[49]). In what follows, we briefly review some of the recent work on such inverse problems. For age-structured population models, several approaches have been developed to recover unknown individual vital rates. For example, in [40, 43] a fixed-point iterative technique was developed to determine the death rate from census data on the age distribution of the population. These studies give conditions on the data that lead to a unique solution. In [26] the authors formulate the inverse problem as an operator equation and then use the least squares method to compute its solution. Because the problem is ill posed, a regularization technique was considered. In addition, the authors prove that the resulting scheme has a convergence rate of the Hölder type. However, no numerical results were reported. A least squares approach was also adopted in [19] for a nonlinear age-structured population model to estimate unknown coefficients from a set of fully discrete observations of the population. Although the convergence of the computed minimizers to a minimizer of the least squares problem was established and numerical results were presented, for many real populations it is generally difficult to obtain discrete observations with respect to age, whereas other quantities, such as total population number, are easily obtained. In [25], a model describing the evolution in time of a size- and age-structured population was considered. A moving finite element method was used to study the identification problem for such a model. Convergence results for the parameter-estimation technique were reported. In [30], by writing a linear age-structured model using the cumulative formulation approach (see, e.g., [24]), the authors studied the inverse problem of identifying the birth and death rates from data on the total population size and the cumulative number of births. They also provided conditions on the data that guarantee the uniqueness of the solution to the inverse problem.

For size-structured population models, the least squares approach has been often used for parameter identification. For example, it was used in [15, 16] to estimate the growth-rate distribution in a linear size-structured population model. A similar technique was subsequently applied to a semilinear size-structured model in [34], where the mortality rate depends on the total population because of competition. In [2], an inverse problem governed by a phytoplankton aggregation model was studied. Convergence and numerical results for identifying the coagulation kernel were provided. Later in [1, 3], this technique was extended to identify parameters in a size-structured population model, where all the individual vital rates (growth, mortality, and reproduction) depend on the total population level. There, these parameters are identified from a set of observations corresponding to the total population number. A finite difference method is then used to approximate the infinite-dimensional problem. Convergence results for the computed parameter estimates to the true parameter are established. To our knowledge, [3] was the first paper to provide convergence results for parameter estimates when the growth rate is a nonlinear function of the total population (i.e., the size-structured model is represented by a *quasi-linear* first-order hyperbolic initial boundary value problem).

In this paper, we extend the discussion in [3] to the following coupled system of quasi-linear size-structured populations model:

$$
\begin{aligned}
&u_t^I + (g^I(x, P(t;q))u^I)_x + m^I(x, P(t;q))u^I = 0, \quad (x,t) \in (0,L] \times (0,T], \\
&g^I(0, P(t;q))u^I(0,t;q) = C^I(t) + \sum_{J=1}^{N} \int_0^L \gamma^{I,J} \beta^J(x, P(t;q))u^J(x,t;q)dx, \quad t \in (0,T], \\
&u^I(x,0;q) = u^{I,0}(x), \quad x \in [0,L].
\end{aligned} \tag{1}
$$

Here $q = (q^1, q^2, \ldots, q^N)$ with $q^I = (g^I, m^I, \beta^I, C^I)$, $I = 1, 2, \ldots, N$, the parameters to be identified. The function $u^I(x,t;q)$, $I = 1, 2, \ldots, N$, is the parameter-dependent size density (number per-unit size) of individuals in the Ith population having size x at time t, and

$$
P(t;q) = \sum_{J=1}^{N} \int_0^L u^J(x,t;q)dx \tag{2}
$$

is the total population at time t. The function g^I denotes the growth rate of an individual in the Ith population, m^I denotes the mortality rate of an individual in the Ith population, and β^I is the reproduction rate of an individual in the Ith population. The function C^I represents the inflow rate of the Ith population of zero-size individuals from an external source (e.g., in a tree population model seeds moved by wind).

The model (1), which was developed by the authors in [4], is a generalization of several size-structured population models (usually referred to as structured models with rate distributions) that have been investigated in [14, 15, 16, 34]. Motivated by the fact that in addition to observable characteristics such as age or size of the individuals, nonobservable genetic characteristics may often play a crucial role in the development of the individuals, researchers in [14] presented the first such generalization of the classic Sinko-Streifer model. This model, a linear version of (1), has vital individual rates that are independent of the total population and distributed over an an infinite-dimensional admissible parameter space with a probability measure. It was shown through numerical simulations in [14] that there is a crucial difference between the dynamics of distributed rate size-structured population models and the classic Sinko-Streifer models. In particular, the classic Sinko-Streifer model cannot have dispersion of the density of the population in age or size except under biologically unreasonable conditions on the growth rate [15]. That is why the classic Sinko-Streifer models conflict with field data collected by experimental biologists. These data sets show that a population with unimodal distribution evolves into a bimodal distribution (see [14] and [41]). In [17], the authors used the least squares approach to fit these distributed rate models to data obtained in [14]. The resulting good fit indicates that the need for such modification is crucial if these models are to be used as prediction tools.

In addition to extending the theory in [3] to the coupled quasi-linear system (1), a main novelty of our current research is that we report on extensive numerical simulations. These simulations are then used to obtain statistical results (in the form of confidence intervals) that provide solid evidence on the feasibility of this approach. It is worth pointing out that with the exception of [28], the above-mentioned articles do not report on any statistical studies.

As the use of numerical methods for estimating functional parameters becomes more widely accepted in the biological sciences, it is becoming increasingly important for investigators to support the efficacy of proposed numerical algorithms with not only numerical simulation results but also confidence intervals on estimated parameters. This can be done by calculating standard errors in a number of sophisticated ways (e.g., pointwise confidence intervals or bands as in [38, 39, 48], uniform bands [32], and simultaneous confidence bands [31]). Here, we simply compute the pointwise standard errors using the pointwise sample variances from a large (1,000) number of inverse problem simulations. While in our efforts we emphasize (regularized) ordinary least square estimators, the ideas and methods presented in this paper can readily be used with maximum-likelihood estimators as well as other standard estimators found in the statistical literature.

It is also worth noting another connection between statistical methods and our efforts in this paper. The models we use here involve a form of "mixing" distributions found in the literature on mixed effects, random effects, or hierarchial methods (see, for example, [20, 21, 22, 35, 36, 46]). However, the models we investigate entail mixing that cannot be decoupled into individual dynamics and thus result in fully coupled dynamics (see section 4).

By a weak solution to problem (1), we mean a bounded and measurable function $u(x,t;q) = (u^1(x,t;q),\, u^2(x,t;q), \dots, u^N(x,t;q))$ satisfying

$$\begin{aligned}
&\int_0^L u^I(x,t;q)\varphi(x,t)dx - \int_0^L u^I(x,0;q)\varphi(x,0)dx \\
&\quad = \int_0^t \int_0^L (u^I\varphi_s + g^I u^I \varphi_x - m^I u^I \varphi) dx\, ds \qquad (3)\\
&\quad + \int_0^t \varphi(0,s)\left(C^I(s) + \sum_{J=1}^N \int_0^L \gamma^{I,J}\beta^J(x,P(s;q))u^J(x,s;q)dx\right) ds
\end{aligned}$$

for $t \in [0,T]$, $I = 1,2,\dots,N$, and every test function $\varphi \in \mathcal{C}^1([0,L]\times[0,T])$.

We first impose a condition on the initial data: for any $I = 1,2,\dots,N$

(H1) $u^{I,0} \in BV[0,L]$ and $u^{I,0}(x) \geq 0$.

Then let $B = \prod_{I=1}^N B^I$ with $B^I = \mathcal{C}^1([0,L];\mathcal{C}_b[0,\infty)) \times \mathcal{C}_b(\Omega) \times \mathcal{C}_b(\Omega) \times \mathcal{C}[0,T]$, where $\Omega = [0,L]\times[0,\infty)$ and $\mathcal{C}_b(\Omega)$ denotes the space of uniformly bounded continuous functions on Ω. We assume that our admissible parameter space Q^I is a compact subset of B^I satisfying (H2)–(H5) below.

(H2) $\beta^I(x,P)$ is a nonnegative Lipschitz continuous function in x and P with a Lipschitz constant L_1. Furthermore, $\beta^I(x,P) \leq \omega_1$, where ω_1 is a positive constant.

(H3) $m^I(x,P)$ is a nonnegative Lipschitz continuous function in x and P with a Lipschitz constant L_2. Furthermore, $m^I(x,P) \leq \omega_2$, where ω_2 is a positive constant.

(H4) $g^I(x,P)$ is twice continuously differentiable with respect to x and satisfies $|g^I(x,P)| + |g^I_x(x,P)| + |g^I_{xx}(x,P)| \leq \omega_3$, where ω_3 is a positive constant. Furthermore, $g^I(x,P) > 0$ for $x \in [0,L)$ and $g^I(L,P) = 0$, and $g^I(x,P)$ and $g^I_x(x,P)$ are Lipschitz continuous in P with a Lipschitz constant L_3.

(H5) $C^I(t)$ is a nonnegative Lipschitz continuous function with a Lipschitz constant L_4.

Let $Q = \prod_{I=1}^{N} Q^I$, then Q is a compact subset of B.

Depending on the values of the constants $0 \le \gamma^{I,J} \le 1$, the model (1) may have two different interpretations. If $\gamma^{I,I} = 1$ and $\gamma^{I,J} = 0,\ I \ne J$, the model represents the dynamics of several populations competing for common resources. On the other hand, if $\gamma^{I,J} > 0$, $I, J = 1, 2, \ldots, N$, then the model may describe the dynamics of one population consisting of N subpopulations, each with its own characteristics. Hence, $\gamma^{I,J}$ represents the probability that an individual of the Jth subpopulation will reproduce an individual of the Ith subpopulation. Therefore, two ways for observing data will be considered. These cause the following two least squares functionals to be minimized: The first is based on the assumption that the model (1) describes N different competing populations. Hence, observations $Z_{I,k}$ (which correspond to the total number of individuals in the Ith population at time t_k) are assumed to be available (this case corresponds to $\gamma^{I,I} = 1$ and $\gamma^{I,J} = 0,\ I \ne J$). We define the least squares cost functional for this case to be

$$\mathcal{J}(q) = \sum_I \sum_k \left| \log\left(\int_0^L u^I(x, t_k; q)dx + 1 \right) - \log(Z_{I,k} + 1) \right|^2, \tag{4}$$

which is minimized over Q. The other case assumes that (1) models one species that has been divided into N not readily distinguishable subpopulations. In this case, we assume that we can only observe aggregate data Z_k, the total number of individuals at time t_k (this case corresponds to $\gamma^{I,J} > 0$, $I, J = 1, 2, \ldots, N$). We define the least squares cost functional

$$\mathcal{J}(q) = \sum_k \left| \log\left(\sum_I \int_0^L u^I(x, t_k; q)dx + 1 \right) - \log(Z_k + 1) \right|^2, \tag{5}$$

which is minimized over Q.

We remark that minimizing (4) over Q is equivalent to the maximum-likelihood estimation of q if

$$\epsilon_{I,k} = \log\left(\int_0^L u^I(x, t_k; q)dx + 1 \right) - \log(Z_{I,k} + 1)$$

are i.i.d.-normal, and minimizing (5) over Q is equivalent to the maximum-likelihood estimation of q if

$$\epsilon_k = \log\left(\sum_I \int_0^L u^I(x, t_k; q)dx + 1 \right) - \log(Z_k + 1)$$

are i.i.d.-normal.

The paper is organized as follows. In section 2, we present a finite difference scheme for computing the solution of (1) and then provide convergence results for the parameter-estimation technique. In section 3, we give ample numerical and statistical results. Section 4 contains some concluding remarks.

2. **Approximation scheme and convergence theory.** The following notation will be used throughout the paper: $\Delta x = L/n$ and $\Delta t = T/l$ denote the spatial and time mesh size, respectively. The mesh points are given by $x_j = j\Delta x, j = 0, 1, 2, \ldots, n$ and $t_k = k\Delta t, k = 0, 1, 2, \ldots, l$. We denote by $u_j^{I,k}(q)$ and $P^k(q)$ the finite difference approximation of $u^I(x_j, t_k; q)$ and $P(t_k; q)$, respectively, and we let

$$g_j^{I,k} = g^I(x_j, P^k(q)),\ \beta_j^{I,k} = \beta^I(x_j, P^k(q)),$$

$$m_j^{I,k} = m^I(x_j, P^k(q)),\ \text{and } C^{I,k} = C^I(t_k).$$

We define the difference operator

$$D_h^-(u_j^{I,k}) = \frac{u_j^{I,k} - u_{j-1}^{I,k}}{\Delta x}, \qquad 1 \le j \le n$$

and the ℓ^1, ℓ^∞ and the BV norms of $u^{I,k}$ by

$$\|u^{I,k}\|_1 = \sum_{j=1}^n |u_j^{I,k}|\triangle x, \quad \|u^{I,k}\|_\infty = \max_{0\le j\le n} |u_j^{I,k}|, \quad \|u^{I,k}\|_{BV} = \sum_{j=1}^n |D_h^-(u_j^{I,k})|\triangle x.$$

We then discretize the partial differential equation in (1) using the following implicit finite difference approximation:

$$\begin{aligned}
&\frac{u_j^{I,k+1}(q) - u_j^{I,k}(q)}{\triangle t} + \frac{g_j^{I,k} u_j^{I,k+1}(q) - g_{j-1}^{I,k} u_{j-1}^{I,k+1}(q)}{\triangle x} + m_j^{I,k} u_j^{I,k+1}(q) = 0,\\
&1 \le j \le n,\\
&g_0^{I,k} u_0^{I,k+1}(q) = C^{I,k} + \sum_{J=1}^N \sum_{j=1}^n \gamma^{I,J} \beta_j^{J,k} u_j^{J,k}(q)\triangle x,\\
&P^{k+1}(q) = \sum_{I=1}^N \sum_{j=1}^n u_j^{I,k+1}(q)\Delta x,
\end{aligned} \tag{6}$$

with the initial condition

$$u_j^{I,0} = \frac{1}{\triangle x} \int_{(j-1)\triangle x}^{j\triangle x} u^{I,0}(x)dx, \qquad j = 1, 2, \ldots, n.$$

If we define

$$d_j^{I,k} = 1 + \frac{\triangle t}{\triangle x} g_j^{I,k} + \triangle t m_j^{I,k}, \qquad j = 1, 2, \ldots, n, \quad I = 1, 2, \ldots, N,$$

then (6) can be equivalently written as the following system of linear equations for

$$\vec{u}^{k+1}(q) = \Big[u_0^{1,k+1}(q), u_1^{1,k+1}(q), \ldots, u_n^{1,k+1}(q), u_0^{2,k+1}(q), u_1^{2,k+1}(q), \ldots, u_n^{2,k+1}(q),$$

$$\ldots, u_0^{N,k+1}(q), u_1^{N,k+1}(q), \ldots, u_n^{N,k+1}(q)\Big]^T \in \mathbb{R}^{N\times(n+1)}$$

$$A^k \vec{u}^{k+1}(q) = \vec{f}^k(q), \tag{7}$$

where

$$\begin{aligned}\vec{f}^k(q) \;=\; \Bigg[& C^{1,k} + \sum_{J=1}^{N}\sum_{j=1}^{n} \gamma^{1,J}\beta_j^{J,k}u_j^{J,k}(q)\triangle x, u_1^{1,k}(q), \ldots, u_n^{1,k}(q), \\ & C^{2,k} + \sum_{J=1}^{N}\sum_{j=1}^{n} \gamma^{2,J}\beta_j^{J,k}u_j^{J,k}(q)\triangle x, u_1^{2,k}(q), \ldots, u_n^{2,k}(q), \ldots, \\ & C^{N,k} + \sum_{J=1}^{N}\sum_{j=1}^{n} \gamma^{N,J}\beta_j^{J,k}u_j^{J,k}(q)\triangle x, u_1^{N,k}(q), \ldots, u_n^{N,k}(q) \Bigg]^T\end{aligned}$$

and A^k is the following block diagonal matrix:

$$A^k = \begin{pmatrix} A^{1,k} & 0 & 0 & \cdots & 0 \\ 0 & A^{2,k} & 0 & \cdots & 0 \\ 0 & 0 & A^{3,k} & \cdots & 0 \\ \cdots & \cdots & \cdots & \cdots & \cdots \\ 0 & 0 & 0 & \cdots & A^{N,k} \end{pmatrix}$$

with the lower triangular matrix

$$A^{I,k} = \begin{pmatrix} g_0^{I,k} & 0 & 0 & \cdots & 0 & 0 \\ -\dfrac{\triangle t}{\triangle x} g_0^{I,k} & d_1^{I,k} & 0 & \cdots & 0 & 0 \\ 0 & -\dfrac{\triangle t}{\triangle x} g_1^{I,k} & d_2^{I,k} & \cdots & 0 & 0 \\ \cdots & \cdots & \cdots & \cdots & \cdots & \cdots \\ 0 & 0 & 0 & \cdots & -\dfrac{\triangle t}{\triangle x} g_{n-1}^{I,k} & d_n^{I,k} \end{pmatrix}.$$

Note that by using the assumptions on our parameters, one can easily show that equation (7) has a unique solution satisfying $\vec{u}^{k+1}(q) \geq 0$, $k = 0, 1, \ldots, l-1$.

The above approximation can be extended to a family of functions $\{U^I_{\Delta x,\Delta t}(x,t;q)\}$ defined by

$$\begin{gathered} U^I_{\Delta x,\Delta t}(x,t;q) = u_j^{I,k}(q) \quad \text{for} \quad (x,t) \in [x_{j-1}, x_j) \times [t_{k-1}, t_k), \\ j = 1, 2, \ldots, n, \quad k = 1, 2, \ldots, l, \quad I = 1, 2, \ldots, N. \end{gathered} \tag{8}$$

Since our parameter set is infinite dimensional, a finite-dimensional approximation of the parameter space is also necessary for computing minimizers. To this end, we consider the following finite-dimensional approximations of (4) and (5), respectively:

$$\mathcal{J}_{\Delta x,\Delta t}(q) = \sum_I \sum_k \left| \log\left(\int_0^L U^I_{\Delta x,\Delta t}(x, t_k; q)dx + 1 \right) - \log(Z_{I,k} + 1) \right|^2 \tag{9}$$

and

$$\mathcal{J}_{\Delta x,\Delta t}(q) = \sum_k \left| \log\left(\sum_I \int_0^L U^I_{\Delta x,\Delta t}(x, t_k; q)dx + 1 \right) - \log(Z_k + 1) \right|^2, \tag{10}$$

each of which is minimized over Q_M, a compact finite-dimensional approximation of the parameter space Q. To establish the convergence results for the parameter-estimation technique, we use an approach similar to that in [3], which is based on the abstract theory in [18].

THEOREM 2.1. *Let $q^i = (q^{1,i}, q^{2,i}, \ldots, q^{N,i})$, and suppose that for each I, $q^{I,i} \to q^I$ in Q^I and $\Delta x_i, \Delta t_i \to 0$ as $i \to \infty$. Let*

$$U_{\Delta x_i,\Delta t_i}(x,t;q^i) = (U^1_{\Delta x_i,\Delta t_i}(x,t;q^i), U^2_{\Delta x_i,\Delta t_i}(x,t;q^i), \ldots, U^N_{\Delta x_i,\Delta t_i}(x,t;q^i))$$

denote the solution of the finite difference scheme, and let

$$u(x,t;q) = (u^1(x,t;q), u^2(x,t;q), \ldots, u^N(x,t;q))$$

be the unique weak solution of our problem with initial condition

$$u^0(x) = (u^{1,0}(x), u^{2,0}(x), \ldots, u^{N,0}(x))$$

and parameter q; then $U^I_{\Delta x_i,\Delta t_i}(x,t;q^i) \to u^I(x,t;q)$ in $\mathcal{L}^1(0,L)$ uniformly in $t \in [0,T]$.

Proof. Define $u_j^{I,k,i} = u_j^{I,k}(q^i)$. From the fact that Q^I is compact and from the results of [4], there exist positive constants c_1, c_2, c_3, and c_4 such that for each $I = 1, 2, \ldots, N$, we have $\sum_{I=1}^{N} \|u^{I,k,i}\|_1 \le c_1$, $\|u^{I,k,i}\|_\infty \le c_2$, $\|u^{I,k,i}\|_{BV} \le c_3$ and $\sum_{j=1}^{n} \left| \frac{u_j^{I,r,i} - u_j^{I,s,i}}{\Delta t_i} \right| \Delta x_i \le c_4(r-s)$, where $r > s$. Thus, for each I there exists a $BV([0,L]\times[0,T])$ function $\hat{u}^I(x,t)$ such that $U^I_{\Delta x_i,\Delta t_i}(x,t;q^i) \to \hat{u}^I(x,t)$ in $\mathcal{L}^1(0,L)$ uniformly in t. Hence, from the uniqueness of bounded variation weak solutions stated in [4], we need only to show that $\hat{u}(x,t) = (\hat{u}^1(x,t), \hat{u}^2(x,t), \ldots, \hat{u}^N(x,t))$ is the weak solution corresponding to the parameter q. To this end, we multiply the first equation of (6) by $\varphi_j^{k+1} = \varphi(x_j, t_{k+1})$, where $\varphi \in \mathcal{C}^1([0,L]\times[0,T])$, to obtain

$$\begin{aligned} &\frac{u_j^{I,k+1,i}\varphi_j^{k+1} - u_j^{I,k,i}\varphi_j^k}{\Delta t_i} - u_j^{I,k,i}\frac{\varphi_j^{k+1} - \varphi_j^k}{\Delta t_i} - g_{j-1}^{I,k,i}u_{j-1}^{I,k+1,i}\frac{\varphi_j^{k+1} - \varphi_{j-1}^{k+1}}{\Delta x_i} \\ &+\frac{g_j^{I,k,i}u_j^{I,k+1,i}\varphi_j^{k+1} - g_{j-1}^{I,k,i}u_{j-1}^{I,k+1,i}\varphi_{j-1}^{k+1}}{\Delta x_i} + m_j^{I,k,i}u_j^{I,k+1,i}\varphi_j^{k+1} = 0. \end{aligned}$$

Multiplying the above equality both sides by $\Delta x_i \Delta t_i$ and summing over $j = 1, 2, \ldots, n$, $k = 0, 1, \ldots, l-1$, we find

$$\begin{aligned} &\sum_{j=1}^{n} \left(u_j^{I,l,i}\varphi_j^l - u_j^{I,0,i}\varphi_j^0 \right) \Delta x_i - \sum_{k=0}^{l-1}\sum_{j=1}^{n} u_j^{I,k,i}\frac{\varphi_j^{k+1} - \varphi_j^k}{\Delta t_i}\Delta x_i \Delta t_i \\ &+ \sum_{k=0}^{l-1} \frac{g_n^{I,k,i}u_n^{I,k+1,i}\varphi_n^{k+1} - g_0^{I,k,i}u_0^{I,k+1,i}\varphi_0^{k+1}}{\Delta x_i}\Delta x_i \Delta t_i \\ &- \sum_{k=0}^{l-1}\sum_{j=1}^{n} g_{j-1}^{I,k,i}u_{j-1}^{I,k+1,i}\frac{\varphi_j^{k+1} - \varphi_{j-1}^{k+1}}{\Delta x_i}\Delta x_i \Delta t_i \\ &+ \sum_{k=0}^{l-1}\sum_{j=1}^{n} m_j^{I,k,i}u_j^{I,k+1,i}\varphi_j^{k+1}\Delta x_i \Delta t_i = 0. \end{aligned}$$

Since $g_n^{I,k,i} = 0$ and $q^{I,i} \to q^I$ as $i \to \infty$ in Q^I, passing to the limit we have

$$\begin{aligned}
&\int_0^L \hat{u}^I(x,t)\varphi(x,t)dx - \int_0^L \hat{u}^I(x,0)\varphi(x,0)dx \\
= \quad &\int_0^t \int_0^L \left(\hat{u}^I\varphi_s + g^I\hat{u}^I\varphi_x - m^I\hat{u}^I\varphi\right) dx\, ds \\
&+ \int_0^t \varphi(0,s)\left(C^I(s) + \sum_{J=1}^N \int_0^L \gamma^{I,J}\beta^J(x,P(s))\hat{u}^J(x,s)dx\right) ds.
\end{aligned}$$

Thus, $\hat{u}(x,t)$ is the weak solution corresponding to the parameter q. $\square$

Since the logarithm function is continuous on $[1,\infty)$, as an immediate consequence of Theorem 2.1, we obtain the following:

Corollary 2.1. *Let $U_{\Delta x,\Delta t}$ denote the numerical solution of (6) with parameter $q^i \to q$ and $\Delta x_i, \Delta t_i \to 0$. Then*

$$\mathcal{J}_{\Delta x_i,\Delta t_i}(q^i) \to \mathcal{J}(q), \quad \text{as } i \to \infty.$$

In the next theorem, we establish the continuity of the approximate cost functional, so that the computational problem of finding the approximate minimizer is well posed.

Theorem 2.2. *Let Δx and Δt be fixed. For each $q^I \in Q^I$, let $U^I_{\Delta x,\Delta t}(x,t;q)$ denote the solution of the finite difference scheme, and $q^{I,i} \to q^I$ as $i \to \infty$ in Q^I; then $U^I_{\Delta x,\Delta t}(x,t;q^i) \to U^I_{\Delta x,\Delta t}(x,t;q)$ as $i \to \infty$ in $\mathcal{L}^1(0,L)$ uniformly in $t \in [0,T]$.*

Proof. Define $\{u_j^{I,k,i}\}$ and $\{u_j^{I,k}\}$ to be the solution of the finite difference scheme with parameter q^i and q, respectively. Let $v_j^{I,k,i} = u_j^{I,k,i} - u_j^{I,k}$; then $v_j^{I,k,i}$ satisfies the following:

$$\begin{aligned}
&\frac{v_j^{I,k+1,i} - v_j^{I,k,i}}{\Delta t} + D_h^-\left[g^{I,i}(x_j,P^{k,i})u_j^{I,k+1,i} - g^I(x_j,P^k)u_j^{I,k+1}\right] \\
&+ m^{I,i}(x_j,P^{k,i})v_j^{I,k+1,i} + \left[m^{I,i}(x_j,P^{k,i}) - m^I(x_j,P^k)\right]u_j^{I,k+1} = 0,
\end{aligned} \tag{11}$$

for $1 \le j \le n$, and

$$\begin{aligned}
&g^{I,i}(0,P^{k,i})u_0^{I,k+1,i} - g^I(0,P^k)u_0^{I,k+1} \\
= \quad &C^{I,i}(t_k) - C^I(t_k) + \sum_{J=1}^N\sum_{j=1}^n \gamma^{I,J}\beta^{J,i}(x_j,P^{k,i})v_j^{J,k,i}\Delta x \\
&+ \sum_{J=1}^N\sum_{j=1}^n \gamma^{I,J}\left[\beta^{J,i}(x_j,P^{k,i}) - \beta^J(x_j,P^k)\right]u_j^{J,k}\Delta x,
\end{aligned} \tag{12}$$

where $P^{k,i}$ denotes $P^k(q^i)$. Multiplying both sides of (11) by $\mathrm{sgn}(v_j^{I,k+1,i})\Delta x$ and summing over $j = 1, 2, \ldots, n$, we obtain

$$\begin{aligned}
&\frac{\|v^{I,k+1,i}\|_1 - \|v^{I,k,i}\|_1}{\Delta t} \\
\leq\ & -\sum_{j=1}^{n} D_h^- \left[g^{I,i}(x_j, P^{k,i}) u_j^{I,k+1,i} - g^I(x_j, P^k) u_j^{I,k+1} \right] \mathrm{sgn}(v_j^{I,k+1,i})\Delta x \\
& -\sum_{j=1}^{n} m^{I,i}(x_j, P^{k,i}) \left| v_j^{I,k+1,i} \right| \Delta x \\
& -\sum_{j=1}^{n} \left[m^{I,i}(x_j, P^{k,i}) - m^I(x_j, P^k) \right] u_j^{I,k+1} \mathrm{sgn}(v_j^{I,k+1,i})\Delta x.
\end{aligned} \tag{13}$$

Using the fact that for any a_j with $a_j \geq 0$, $j = 0, 1, 2, \ldots, n$, we have

$$\sum_{j=1}^{n} D_h^- (a_j b_j) \mathrm{sgn}(b_j)\Delta x \geq a_n |b_n| - a_0 |b_0|,$$

and we obtain

$$\begin{aligned}
& -\sum_{j=1}^{n} D_h^- \left[g^{I,i}(x_j, P^{k,i}) u_j^{I,k+1,i} - g^I(x_j, P^k) u_j^{I,k+1} \right] \mathrm{sgn}(v_j^{I,k+1,i})\Delta x \\
=\ & -\sum_{j=1}^{n} D_h^- \left(g^{I,i}(x_j, P^{k,i}) v_j^{I,k+1,i} \right) \mathrm{sgn}(v_j^{I,k+1,i})\Delta x \\
& -\sum_{j=1}^{n} D_h^- \left[\left((g^{I,i}(x_j, P^{k,i}) - g^I(x_j, P^k) \right) u_j^{I,k+1} \right] \mathrm{sgn}(v_j^{I,k+1,i})\Delta x \\
\leq\ & g^{I,i}(0, P^{k,i}) |v_0^{I,k+1,i}| + \sup_{1 \leq j \leq n} \left| g^{I,i}(x_j, P^{k,i}) - g^I(x_j, P^k) \right| \|u^{I,k+1}\|_{BV} \\
& + \sup_{1 \leq j \leq n} \left| D_h^- \left(g^{I,i}(x_j, P^{k,i}) - g^I(x_j, P^k) \right) \right| \left(\|u^{I,k+1}\|_\infty + (\|u^{I,k+1}\|_1 \right).
\end{aligned} \tag{14}$$

By (12), we have

$$\begin{aligned}
& g^{I,i}(0, P^{k,i}) |v_0^{I,k+1,i}| \\
\leq\ & \left| g^{I,i}(0, P^{k,i}) - g^I(0, P^k) \right| u_0^{I,k+1} + \left| C^{I,i}(t_k) - C^I(t_k) \right| \\
& + \omega_1 \sum_{J=1}^{N} \|v^{J,k,i}\|_1 + \max_{1 \leq J \leq N} \sup_{1 \leq j \leq n} \left| \beta^{J,i}(x_j, P^{k,i}) - \beta^J(x_j, P^k) \right| \sum_{J=1}^{N} \|u^{J,k}\|_1.
\end{aligned} \tag{15}$$

Summing (13) over $I = 1, 2, \ldots, N$, and using (14) and (15), we obtain

$$
\begin{aligned}
&\frac{\sum_{I=1}^{N} \|v^{I,k+1,i}\|_1 - \sum_{I=1}^{N} \|v^{I,k,i}\|_1}{\Delta t} \\
\leq\ & \max_{1\leq I\leq N} \sup_{1\leq j\leq n} \left| D_h^- \left(g^{I,i}(x_j, P^{k,i}) - g^I(x_j, P^k) \right) \right| \sum_{I=1}^{N} \|u^{I,k+1}\|_1 \\
&+N \max_{1\leq I\leq N} \sup_{1\leq j\leq n} \left| D_h^- \left(g^{I,i}(x_j, P^{k,i}) - g^I(x_j, P^k) \right) \right| \max_{1\leq I\leq N} \|u^{I,k+1}\|_\infty \\
&+N \max_{1\leq I\leq N} \sup_{1\leq j\leq n} \left| g^{I,i}(x_j, P^{k,i}) - g^I(x_j, P^k) \right| \max_{1\leq I\leq N} \|u^{I,k+1}\|_{BV} \\
&+N \max_{1\leq I\leq N} \left| g^{I,i}(0, P^{k,i}) - g^I(0, P^k) \right| \max_{1\leq I\leq N} \|u^{I,k+1}\|_\infty \\
&+N \max_{1\leq J\leq N} \sup_{1\leq j\leq n} \left| \beta^{J,i}(x_j, P^{k,i}) - \beta^J(x_j, P^k) \right| \sum_{J=1}^{N} \|u^{J,k}\|_1 \\
&+N \max_{1\leq I\leq N} \left| C^{I,i}(t_k) - C^I(t_k) \right| + N\omega_1 \sum_{I=1}^{N} \|v^{I,k,i}\|_1 \\
&+ \max_{1\leq I\leq N} \sup_{1\leq j\leq n} \left| m^{I,i}(x_j, P^{k,i}) - m^I(x_j, P^k) \right| \sum_{I=1}^{N} \|u^{I,k+1}\|_1.
\end{aligned}
$$

Noting that

$$
\begin{aligned}
& \left| g^{I,i}(x_j, P^{k,i}) - g^I(x_j, P^k) \right| \\
\leq\ & \left| g^{I,i}(x_j, P^{k,i}) - g^{I,i}(x_j, P^k) \right| + \left| g^{I,i}(x_j, P^k) - g^I(x_j, P^k) \right|,
\end{aligned}
$$

we have from (H4) the following:

$$
\begin{aligned}
& \max_{1\leq I\leq N} \sup_{1\leq j\leq n} \left| g^{I,i}(x_j, P^{k,i}) - g^I(x_j, P^k) \right| \\
\leq\ & L_3 \sum_{I=1}^{N} \|v^{I,k,i}\|_1 + \max_{1\leq I\leq N} \sup_{1\leq j\leq n} \left| g^{I,i}(x_j, P^k) - g^I(x_j, P^k) \right|.
\end{aligned}
$$

Similarly, we can show that

$$
\begin{aligned}
& \max_{1\leq I\leq N} \sup_{1\leq j\leq n} \left| \beta^{I,i}(x_j, P^{k,i}) - \beta^I(x_j, P^k) \right| \\
\leq\ & L_1 \sum_{I=1}^{N} \|v^{I,k,i}\|_1 + \max_{1\leq I\leq N} \sup_{1\leq j\leq n} \left| \beta^{I,i}(x_j, P^k) - \beta^I(x_j, P^k) \right|
\end{aligned}
$$

and

$$
\begin{aligned}
& \max_{1\leq I\leq N} \sup_{1\leq j\leq n} \left| m^{I,i}(x_j, P^{k,i}) - m^I(x_j, P^k) \right| \\
\leq\ & L_2 \sum_{I=1}^{N} \|v^{I,k,i}\|_1 + \max_{1\leq I\leq N} \sup_{1\leq j\leq n} \left| m^{I,i}(x_j, P^k) - m^I(x_j, P^k) \right|.
\end{aligned}
$$

Furthermore, straightforward computations yield

$$
\begin{aligned}
&\left|D_h^-\left[g^{I,i}(x_j,P^{k,i})-g^I(x_j,P^k)\right]\right| \\
=\ &\left|\frac{1}{\Delta x}\int_0^1 \frac{d}{dr}\left(g^{I,i}(rx_j+(1-r)x_{j-1},P^{k,i})-g^I(rx_j+(1-r)x_{j-1},P^k)\right)dr\right| \\
=\ &\left|\int_0^1 g_x^{I,i}(rx_j+(1-r)x_{j-1},P^{k,i})dr-\int_0^1 g_x^I(rx_j+(1-r)x_{j-1},P^k)dr\right| \\
\leq\ &\int_0^1 \left|g_x^{I,i}(rx_j+(1-r)x_{j-1},P^{k,i})-g_x^{I,i}(rx_j+(1-r)x_{j-1},P^k)\right|dr \\
&+\int_0^1 \left|g_x^{I,i}(rx_j+(1-r)x_{j-1},P^k)-g_x^I(rx_j+(1-r)x_{j-1},P^k)\right|dr.
\end{aligned}
$$

Hence, from (H4) we obtain

$$
\begin{aligned}
&\max_{1\leq I\leq N}\sup_{1\leq j\leq n}\left|D_h^-\left[g^{I,i}(x_j,P^{k,i})-g^I(x_j,P^k)\right]\right| \\
\leq\ & L_3\sum_{I=1}^N\|v^{I,k,i}\|_1+\max_{1\leq I\leq N}\sup_{1\leq j\leq n}\int_0^1\left|g_x^{I,i}(\bar{x}_j,P^k)-g_x^I(\bar{x}_j,P^k)\right|dr,
\end{aligned}
$$

where $\bar{x}_j=rx_j+(1-r)x_{j-1}$. Set

$$
\begin{aligned}
\delta_k\ =\ & L_3\left(N\max_{1\leq I\leq N}\|u^{I,k+1}\|_\infty+\sum_{I=1}^N\|u^{I,k+1}\|_1\right)+NL_1\sum_{I=1}^N\|u^{I,k}\|_1+N\omega_1 \\
&+NL_3\left(\max_{1\leq I\leq N}\|u^{I,k+1}\|_{BV}+\max_{1\leq I\leq N}\|u^{I,k+1}\|_\infty\right)+L_2\sum_{I=1}^N\|u^{I,k+1}\|_1
\end{aligned}
$$

and

$$
\begin{aligned}
\rho_{k,i}\ =\ & \sum_{I=1}^N\|u^{I,k+1}\|_1\max_{1\leq I\leq N}\sup_{1\leq j\leq n}\int_0^1\left|g_x^{I,i}(\bar{x}_j,P^k)-g_x^I(\bar{x}_j,P^k)\right|dr \\
&+N\max_{1\leq I\leq N}\|u^{I,k+1}\|_\infty\max_{1\leq I\leq N}\sup_{1\leq j\leq n}\int_0^1\left|g_x^{I,i}(\bar{x}_j,P^k)-g_x^I(\bar{x}_j,P^k)\right|dr \\
&+N\max_{1\leq I\leq N}\|u^{I,k+1}\|_{BV}\max_{1\leq I\leq N}\sup_{1\leq j\leq n}\left|g^{I,i}(x_j,P^k)-g^I(x_j,P^k)\right| \\
&+N\max_{1\leq I\leq N}\|u^{I,k+1}\|_\infty\max_{1\leq I\leq N}\left|g^{I,i}(0,P^k)-g^I(0,P^k)\right| \\
&+N\sum_{I=1}^N\|u^{I,k}\|_1\max_{1\leq I\leq N}\sup_{1\leq j\leq n}\left|\beta^{I,i}(x_j,P^k)-\beta^I(x_j,P^k)\right| \\
&+N\max_{1\leq I\leq N}\left|C^{I,i}(t_k)-C^I(t_k)\right| \\
&+\sum_{I=1}^N\|u^{I,k+1}\|_1\max_{1\leq I\leq N}\sup_{1\leq j\leq n}\left|m^{I,i}(x_j,P^k)-m^I(x_j,P^k)\right|.
\end{aligned}
$$

Then, we have

$$
\frac{\sum_{I=1}^N\|v^{I,k+1,i}\|_1-\sum_{I=1}^N\|v^{I,k,i}\|_1}{\Delta t}\leq\delta_k\sum_{I=1}^N\|v^{I,k,i}\|_1+\rho_{k,i}.
$$

Since for each k, $\rho_{k,i} \to 0$ as $i \to \infty$, the desired result easily follows from this inequality. □

THEOREM 2.3. *Suppose that Q_M is a sequence of compact subsets of Q. Moreover, assume that for each $q \in Q$, there exists a sequence of $q_M \in Q_M$ such that $q_M \to q$ as $M \to \infty$. Then the functional $\mathcal{J}_{\Delta x,\Delta t}$ has a minimizer over Q_M. Furthermore, if q_M^i denotes a minimizer of $\mathcal{J}_{\Delta x_i,\Delta t_i}$ over Q_M and $\Delta x_i, \Delta t_i \to 0$, then any subsequence of q_M^i has a further subsequence which converges to a minimizer of $\mathcal{J}$.*

Proof. The proof of this theorem is a direct application of the abstract theory in [18], based on the convergence of $\mathcal{J}_{\Delta x_i,\Delta t_i}(q^i) \to \mathcal{J}(q)$. □

3. **Numerical results.** In this section, we present numerical simulations and statistical results. In all of the simulations below, we assume $L = 1$, $T = 1$, and $C^I(t) = 0$ for $I = 1, 2, \ldots, N$.

In sections 3.1 and 3.2, we assume $N = 1$ and that all the parameters are known except for β. To estimate β, we use data that are generated computationally as follows: Let

$$u^0(x) = 3\exp(-2(x-0.5)^2), \quad g(x,P) = 5(1-x)\exp(-3P),$$
$$m(x,P) = \exp(4(x-0.4)^2)\exp(0.2P), \quad \beta(x,P) = 6x(1-x)\exp(-3P),$$

and we solve (6) and (8) for $U_{\Delta x,\Delta t}(x,t)$. We set $Z_k = (1+\varepsilon_k)\int_0^1 U_{\Delta x,\Delta t}(x,t_k)dx$, where ε_k is a random sample from a normal random number generator with mean zero and standard deviation $\sigma = 0.02$.

3.1. **$1-$D linear estimation problem for finite-dimensional parameter space when $N = 1$.** In our first example, we assume that β is of a separable form given by $\beta(x,P) = b(x)\exp(-3P)$, where $b(x) = \mu x(1-x^\nu)$ with μ and ν two unknown constants to be identified. Hence, the solution to our least squares problems involves identifying the two constants μ and ν from a compact subset of $\mathbb{R}_+^2$ so as to minimize the least squares cost functional

$$\mathcal{J}_{\Delta x,\Delta t}(q) = \sum_{k=1}^{m} \left| \log\left(\int_0^1 U_{\Delta x,\Delta t}(x,t_k;q)dx + 1 \right) - \log(Z_k+1) \right|^2.$$

To test the performance of the parameter-estimation technique when no infinite-dimensional effects are present, in Figure 1 we choose $\Delta x = \Delta t = 0.005$ both for generating the data and for the numerical solution (8) in the least squares problem. This avoids the infinite-dimensional effect of the partial differential equation given in (1). In fact, if the noise is removed from the data, and the parameters μ and ν are known, then numerically solving our model produces the exact data.

In Figure 2, we use $\Delta x = \Delta t = 0.005$ to generate the data while we use $\Delta x = \Delta t = 0.01$ for the numerical solution (8) in the least squares problem. Thus, in this case the data are not exactly attained by our model, even if the noise is removed (an error is present due to the finite-dimensional approximation of our infinite-dimensional model). The results of Figure 2 are obtained by using the same values for the rest of the parameters as those of Figure 1.

A similar format for presenting the results of 1,000 inverse problem calculations was used in Figures 1 and 2. The left part of each of the figures represents the S (for our case $S = 1,000$) numerical results for the estimated parameter $b^s(x)$ $(s = 1, 2, \ldots, S)$ versus the exact $b(x)$, where these 1,000 distinct numerical results graphed were obtained by solving 1,000 inverse problems, each of which corresponds to a given noise sample $\{\epsilon_k\}$. The right part represents the figure of the corresponding 95% confidence interval (dashed line) versus the exact $b(x)$ (solid line), where the 95% confidence interval is obtained by choosing the band between the upper 2.5% and lower 2.5% of these 1,000 numerical results. Table 1 provides statistical results for the corresponding graphs, where $AB(x) = \frac{1}{S}\sum_{s=1}^{S}(b^s(x) - b(x))$ denotes the average bias for all approximations at x, $RAB(x) = 100\frac{AB(x)}{b(x)}$ denotes the relative average bias for all approximations at x, and

$$SE(x) = \left[\frac{1}{S-1}\sum_{s=1}^{S}(b^s(x) - b(x) - AB(x))^2\right]^{\frac{1}{2}}$$

denotes the sampling standard error at the point x. Note that this is simply the usual asymptotic formula for the pointwise standard error (e.g., see [21, pp. 28, 37] and [45, p. 308]).

Although the estimates in both figures are good, the results in Figures 1 and 2 and Table 1 suggest that infinite-dimensional effects can lead to a slightly underbiased estimator. We suspect this bias depends on the choice of the numerical scheme used for solving the infinite-dimensional partial differential equation model. Here, we are using an upwind scheme for approximating the model and a right-hand sum for approximating all the integrals involved. This biased estimator may be improved if, for example, a centered finite difference approximation is used together with a trapezoidal rule for integration.

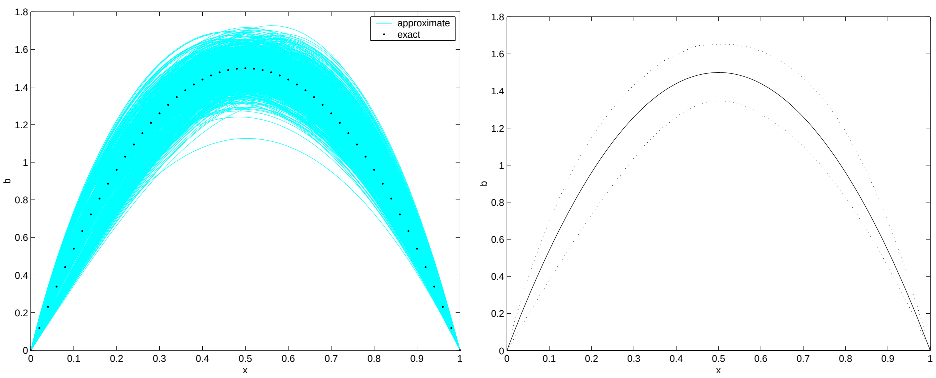

FIGURE 1. $\Delta x = \Delta t = 0.005$ to generate the data and solve the least squares. For the left part of the figure, each of the grey lines (....) denotes a distinct result for a given sample $\{\epsilon_k\}$.

The above statistical results (essentially on how measurement error affects estimates) are based on a large number of numerical simulations (somewhat in the spirit of Bayesian-based MCMC calculations used to estimate means and variances in a probability distribution from "experimental" data). Any estimate of model parameters from data can also be accompanied by an estimate of uncertainty using standard regression formulations from statistics [21]. Thus, in the remaining part

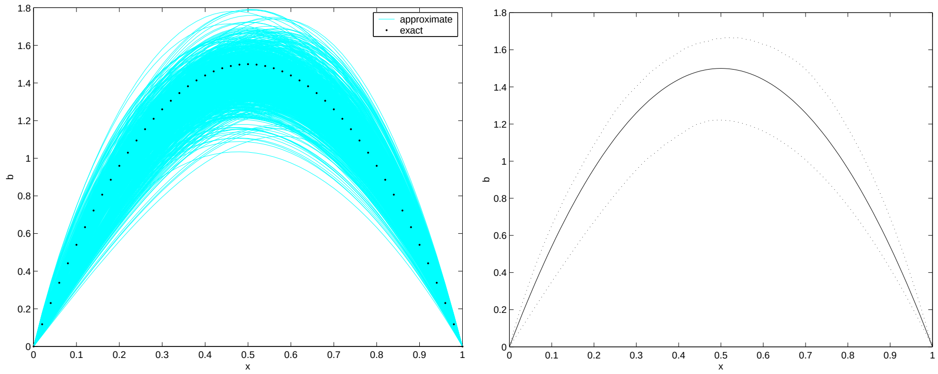

FIGURE 2. $\Delta x = \Delta t = 0.005$ to generate the data and $\Delta x = \Delta t = 0.01$ to solve the least squares. For the left part of the figure, each of the grey lines (....) denotes a distinct result for a given sample $\{\epsilon_k\}$.

TABLE 1. Statistical results for Figures 1 and 2

Figure 1				Figure 2			
x	$AB(x)$	$RAB(x)$	$SE(x)$	x	$AB(x)$	$RAB(x)$	$SE(x)$
0.1	-0.0037	-0.6870	0.0749	0.1	-0.0390	-7.2314	0.0747
0.2	-0.0092	-0.9580	0.0993	0.2	-0.0651	-6.7812	0.1053
0.3	-0.0107	-0.8463	0.0975	0.3	-0.0768	-6.0949	0.1130
0.4	-0.0079	-0.5497	0.0860	0.4	-0.0763	-5.2995	0.1124
0.5	-0.0021	-0.1427	0.0798	0.5	-0.0666	-4.4422	0.1138
0.6	0.0049	0.3378	0.0852	0.6	-0.0511	-3.5460	0.1188
0.7	0.0110	0.8707	0.0926	0.7	-0.0331	-2.6236	0.1202
0.8	0.0138	1.4425	0.0882	0.8	-0.0162	-1.6830	0.1075
0.9	0.0110	2.0444	0.0605	0.9	-0.0039	-0.7294	0.0706

of this subsection, we present a statistically based method to actually compute the variance in the estimated model parameters $q = (\mu,\ \nu)$.

To perform this analysis, we need to compute the sensitivity matrix

$$X(q) = \begin{bmatrix} \dfrac{P_\mu(t_1;q)}{1+P(t_1;q)} & \dfrac{P_\nu(t_1;q)}{1+P(t_1;q)} \\ \dfrac{P_\mu(t_2;q)}{1+P(t_2;q)} & \dfrac{P_\nu(t_2;q)}{1+P(t_2;q)} \\ \cdots & \cdots \\ \dfrac{P_\mu(t_m;q)}{1+P(t_m;q)} & \dfrac{P_\nu(t_m;q)}{1+P(t_m;q)} \end{bmatrix}. \tag{16}$$

Note that we cannot compute $P(t;q)$, $P_\mu(t;q)$, or $P_\nu(t;q)$ directly from our model. Therefore, we use the difference scheme (6) to obtain the following approximation of $P(t;q)$:

$$\widehat{P}(t;q) = \int_0^1 U_{\Delta x,\Delta t}(x,t;q)dx.$$

Then, we use a forward difference approximation for the derivative $P_\mu(t;q)$ and $P_\nu(t;q)$ given by

$$\widehat{P}_\mu(t;\mu,\nu) = \frac{1}{\Delta\mu}\left(\widehat{P}(t;\mu+\Delta\mu,\nu) - \widehat{P}(t;\mu,\nu)\right)$$

and

$$\widehat{P}_\nu(t;q) = \frac{1}{\Delta\nu}\left(\widehat{P}(t;\mu,\nu+\Delta\nu) - \widehat{P}(t;\mu,\nu)\right).$$

Substituting $\widehat{P}(t_i;q)$, $\widehat{P}_\mu(t_i;q)$, and $\widehat{P}_\nu(t_i,q)$ for $P(t_i;q)$, $P_\mu(t_i;q)$, and $P_\nu(t_i;q)$ in (16), respectively, we obtain the following approximation of $X(q)$:

$$\widehat{X}(q) = \begin{bmatrix} \dfrac{\widehat{P}_\mu(t_1;q)}{1+\widehat{P}(t_1;q)} & \dfrac{\widehat{P}_\nu(t_1;q)}{1+\widehat{P}(t_1;q)} \\ \dfrac{\widehat{P}_\mu(t_2;q)}{1+\widehat{P}(t_2;q)} & \dfrac{\widehat{P}_\nu(t_2;q)}{1+\widehat{P}(t_2;q)} \\ \cdots & \cdots \\ \dfrac{\widehat{P}_\mu(t_m;q)}{1+\widehat{P}(t_m;q)} & \dfrac{\widehat{P}_\nu(t_m;q)}{1+\widehat{P}(t_m;q)} \end{bmatrix}.$$

Under standard assumptions of classic nonlinear regression theory, we know that if $\hat{\epsilon}_i \sim \mathcal{N}(0,\sigma^2)$, where $\hat{\epsilon}_i$ is the difference between observation and model at time t_i, then the least squares estimate q^* is expected to be asymptotically normally distributed. In particular, for large samples, we may assume

$$q^* \sim \mathcal{N}[q_0, \sigma^2\{X^T(q_0)X(q_0)\}^{-1}], \tag{17}$$

where q_0 is the true vector of parameters and $\sigma^2\{X^T(q_0)X(q_0)\}^{-1}$ is the true covariance matrix (see [21, chap. 2]).

Since q_0 and σ^2 are not available, we follow a standard statistical practice [5]: substitute the computed estimate q^* for q_0 and approximate σ^2 by

$$\hat{\sigma}^2 = \frac{1}{m-2}\sum_{j=1}^{m}\left(\log\left(\widehat{P}(t_j;q^*)+1\right) - \log(Z_j+1)\right)^2 \tag{18}$$

in (17) to obtain the standard deviation for our estimates. In particular, if

$$V = \hat{\sigma}^2\{\widehat{X}^T(q^*)\widehat{X}(q^*)\}^{-1} = \begin{bmatrix} V_{11} & V_{12} \\ V_{21} & V_{22} \end{bmatrix},$$

then we take $\sqrt{V_{11}}$ and $\sqrt{V_{22}}$ to be the standard deviation for parameters μ and ν, respectively. The following two tables are the standard deviation of μ and ν for the results of the first eight numerical simulations of Figures 1 and 2, respectively.

TABLE 2. Standard deviation for the results of the first eight numerical simulations in Figure 1

μ	1.1613	1.0494	1.0451	1.1109	1.0864	1.4684	1.1605	1.0512
ν	1.2124	0.3073	0.2999	0.2741	0.2701	1.5555	0.2482	0.2390

Table 4 provides the average standard deviation of μ and ν for the results of all the 1,000 numerical simulations of Figures 1 and 2, respectively. We note that in most practical situations using experimental data, one does not expect to have 1,000 experiments performed. But the above procedures will produce estimates of variances even with only a single data set.

TABLE 3. Standard deviation for the results of the first eight numerical simulations in Figure 2

μ	1.7066	1.5636	1.6192	1.7974	1.6389	2.8009	1.8619	1.3893
ν	0.7716	0.3238	0.4838	0.1812	0.3426	2.8685	0.3828	0.4136

TABLE 4. Average of standard deviation for all the results of the numerical simulations in Figures 1 and 2

	Figure 1	Figure 2
μ	1.1921	1.9197
ν	0.4566	0.8572

3.2. **$1-$D linear estimation problem for infinite-dimensional parameter space when $N = 1$.** In this example, we assume that β is of a separable form given by $\beta(x,P) = b(x)\exp(-3P)$, where $b(x)$ is an unknown parameter that we want to identify.

Let

$$\mathcal{D} = \{f \in \mathcal{C}[0,1] : |f(x) - f(y)| \leq K|x-y|, f(0) = f(1) = 0\}.$$

Choose the parameter space $Q = \mathcal{D}$. Clearly, by the Arzela-Ascoli theorem [33], Q is compact in $\mathcal{C}[0,1]$. We approximate the infinite-dimensional parameter space as follows: For M, a positive integer, and $b \in Q$, we set

$$(\mathcal{I}_M b)(x) = \sum_{i=1}^{M-1} b\left(\frac{i}{M}\right)\phi_M^i(x;0,1),$$

where $\phi_M^i(x;0,1)$ are the linear spline functions on a uniform mesh of the interval $[0,1]$. These are defined by

$$\phi_M^i(x;0,1) = \begin{cases} 1 - i + \dfrac{x}{h}, & (i-1)h \leq x \leq ih, \\ 1 + i - \dfrac{x}{h}, & ih \leq x \leq (i+1)h, \qquad i = 1,2,\ldots,M-1, \\ 0, & |x - ih| \geq h, \end{cases}$$

where $h = \dfrac{1}{M}$. It can be readily argued that $\lim_{M\to\infty} \mathcal{I}_M b = b$ in $\mathcal{C}[0,1]$, uniformly in b [44]. Hence, if $b_M \in Q_M = \mathcal{I}_M(Q)$ is given by

$$b_M(x) = \sum_{i=1}^{M-1} \lambda_M^i \phi_M^i(x;0,1),$$

then the solution of our finite-dimensional identification problem involves identifying the $M-1$ coefficients $\{\lambda_M^i\}_{i=1}^{M-1}$ from a compact subset of $\mathbb{R}_+^{M-1}$ so as to minimize the least squares cost functional (9).

To indirectly implement the compactness constraints of Q, we use a regularized least squares cost functional of the form

$$\begin{aligned}\mathcal{J}_{\Delta x,\Delta t}(q) &= \sum_{k=1}^{m}\left|\log\left(\int_0^1 U_{\Delta x,\Delta t}(x,t_k;q)dx+1\right)-\log(Z_k+1)\right|^2\\ &\quad +\alpha\int_0^1\left|\frac{d}{dx}b_M(x)\right|^2 dx,\end{aligned}$$

where $\alpha > 0$ is the regularization parameter.

The left part of each of the following figures again represents the S (=1,000) numerical results of the estimated parameter versus the exact parameter $b(x)$. The right part represents the figure of the corresponding 95% confidence interval (dashed line) versus the exact $b(x)$ (solid line). The tables provide statistical results for the corresponding graphs.

3.2.1. *Effect of infinite-dimensional model on parameter estimate.* In Figure 3, we use $\Delta x = 0.005$ and $\Delta t = 0.005$ to generate the data and the numerical solution (8) for the least squares problem. This removes the infinite-dimensional effect of the partial differential equation given by (1). However, in Figure 4, we use $\Delta x = \Delta t = 0.005$ to generate the data and $\Delta x = \Delta t = 0.01$ to compute (8). Thus, in this case the data are not exactly attained by our model even if the noise is removed. We observe that while the estimates in both figures are good, the results in Figures 3 and 4 and Table 5 suggest that infinite-dimensional effects can lead to a slightly underbiased estimator.

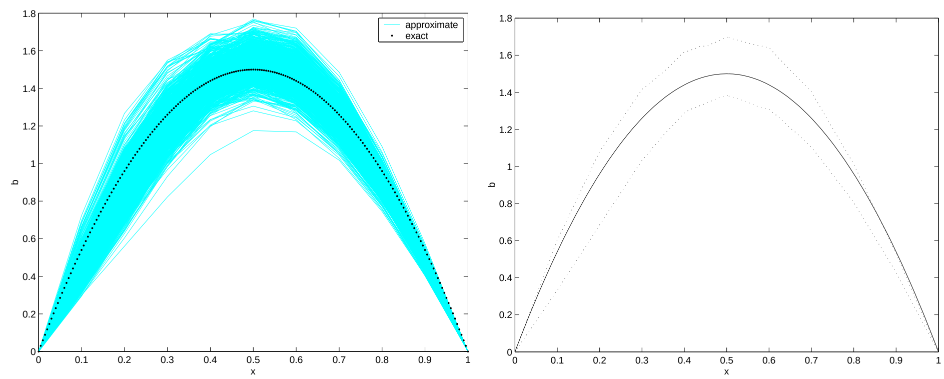

FIGURE 3. $M = 10$, $\alpha = 3e-5$. Each of the grey lines (....) of the left part of the figure denotes a distinct result for a given sample $\{\epsilon_k\}$.

3.2.2. *Effect of regularization parameter α on parameter estimate.* In Figures 5 and 6, we change the parameter α while keeping the rest fixed. Clearly, the low regularization parameter leads to relatively bad estimates, although the estimator in this case seems to be the least biased (see Figure 5 and left part of Table 6). Increasing the value of α leads to better parameter estimates, but the estimator becomes more underbiased (see Figure 6 and right part of Table 6). If this value is increased further, the estimator is more biased, and the parameter estimate becomes less accurate than before. This suggests, not surprisingly, that there is an

TABLE 5. Statistical results for Figures 3 and 4

Figure 3				Figure 4			
x	$AB(x)$	$RAB(x)$	$SE(x)$	x	$AB(x)$	$RAB(x)$	$SE(x)$
0.1	-0.0778	-14.4108	0.0723	0.1	-0.1236	-22.8940	0.0667
0.2	-0.0816	-8.5015	0.1070	0.2	-0.1571	-16.3628	0.1040
0.3	-0.0400	-3.1727	0.1012	0.3	-0.1284	-10.1885	0.1141
0.4	0.0110	0.7636	0.0834	0.4	-0.0785	-5.4485	0.1130
0.5	0.0386	2.5745	0.0818	0.5	-0.0440	-2.9329	0.1110
0.6	0.0283	1.9621	0.0868	0.6	-0.0446	-3.0966	0.1049
0.7	-0.0124	-0.9880	0.0779	0.7	-0.0754	-5.9875	0.0885
0.8	-0.0559	-5.8206	0.0556	0.8	-0.1059	-11.0334	0.0624
0.9	-0.0623	-11.5426	0.0280	0.9	-0.0939	-17.3949	0.0323

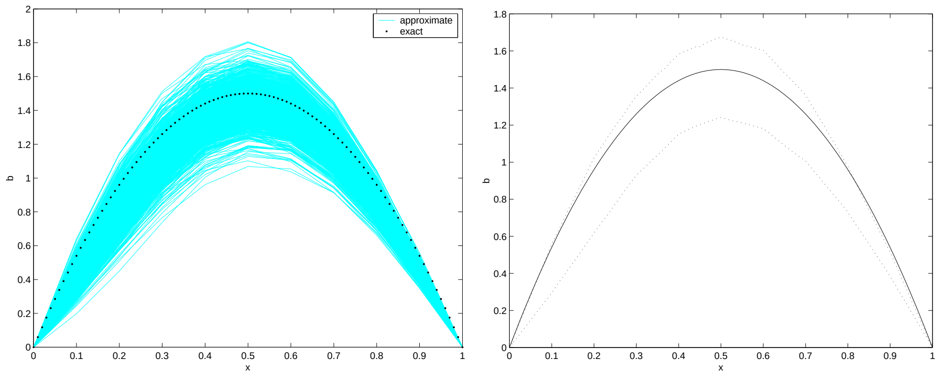

FIGURE 4. $M = 10$, $\alpha = 3e-5$. Each of the grey lines (....) of the left part of the figure denotes a distinct result for a given sample $\{\epsilon_k\}$.

optimal choice for the parameter α that produces the best results for the parameter estimates.

TABLE 6. Statistical results for Figures 5 and 6

Figure 5				Figure 6			
x	$AB(x)$	$RAB(x)$	$SE(x)$	x	$AB(x)$	$RAB(x)$	$SE(x)$
0.1	-0.1277	-23.6389	0.1206	0.1	-0.1241	-22.9816	0.0506
0.2	-0.1648	-17.1644	0.1791	0.2	-0.1621	-16.8881	0.0842
0.3	-0.1284	-10.1938	0.1618	0.3	-0.1432	-11.3627	0.1011
0.4	-0.0599	-4.1591	0.1221	0.4	-0.1050	-7.2906	0.1078
0.5	-0.0072	-0.4806	0.1169	0.5	-0.0791	-5.2736	0.1087
0.6	0.0026	0.1788	0.1274	0.6	-0.0837	-5.8139	0.1009
0.7	-0.0253	-2.0101	0.1126	0.7	-0.1077	-8.5443	0.0847
0.8	-0.0631	-6.5678	0.0780	0.8	-0.1288	-13.4165	0.0602
0.9	-0.0642	-11.8944	0.0427	0.9	-0.1042	-19.3027	0.0313

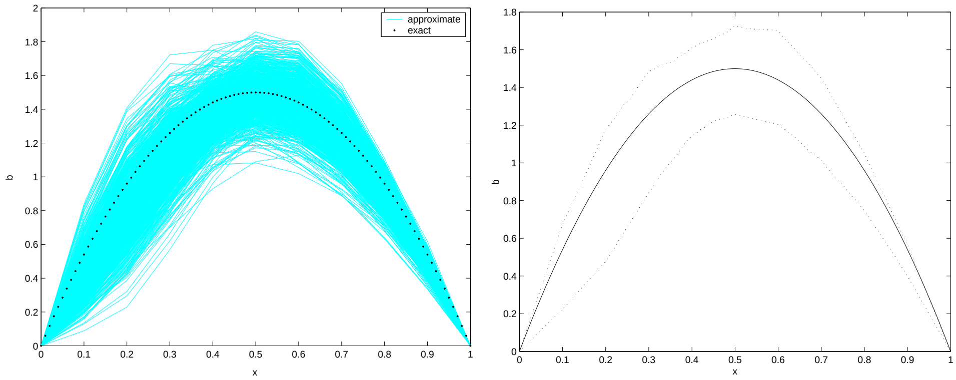

FIGURE 5. $M = 10$, $\alpha = 1e-5$. Each of the grey lines (....) of the left part of the figure denotes a distinct result for a given sample $\{\epsilon_k\}$.

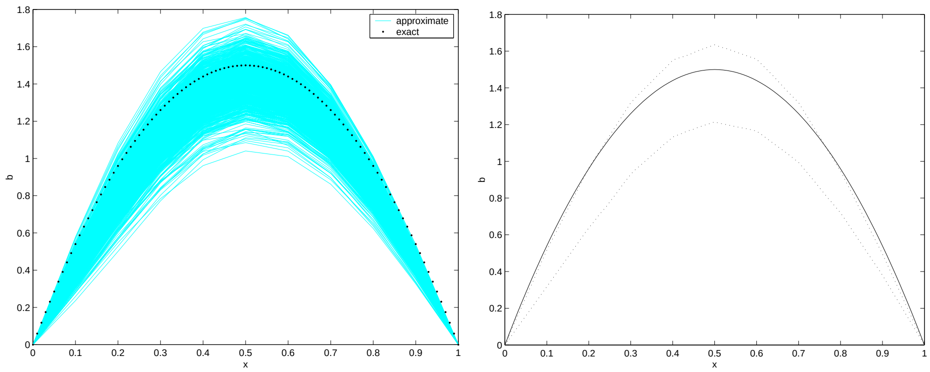

FIGURE 6. $M = 10$, $\alpha = 5e-5$. Each of the grey lines (....) of the left part of the figure denotes a distinct result for a given sample $\{\epsilon_k\}$.

3.3. **$\mathbf{1-D}$ linear estimation problem for infinite-dimensional parameter space when $\mathbf{N = 2}$.** In this section, we assume $N = 2$ and that all the parameters are known except for β^1 and β^2. To estimate β^1 and β^2, we assume that they are of a separable form given by $\beta^1(x, P) = b^1(x)\exp(-P)$ and $\beta^2(x, P) = b^2(x)\exp(-P)$, respectively, where $b^1(x)$ and $b^2(x)$ are unknown parameters to be identified. To estimate $b^1(x)$ and $b^2(x)$, we use data that are generated computationally as follows: Let $\gamma^{I,J} = \begin{cases} 1, & I = J \\ 0, & I \neq J \end{cases}$ for Figure 7 and $\gamma^{I,J} = 0.5$, $I, J = 1, 2$ for Figure 8, $u^{I,0}(x) = 3\exp(-2(x - 0.1)^2)$, and for the parameters g^I, m^I, and β^I, we use the following choice of functions:

$$
\begin{aligned}
&g^1 = 2(1 - x)\exp(-0.8P), \quad g^2 = (1 - x)(1 + 2P)\exp(-P),\\
&m^1 = \exp(2(x - 0.4)^2)\exp(0.2P), \quad m^2 = \exp(2(x - 0.4)^2)\exp(0.2P),\\
&\beta^1 = 6(1 - x)x\exp(-P), \quad \beta^2 = 6(1 - x)x\exp(-5(x - 0.5)^2)\exp(-P),
\end{aligned}
$$

and solve (1) for $U^I_{\Delta x,\Delta t}(x,t)$, $I=1,2$. We set $Z_{I,k}=(1+\varepsilon_{I,k})\int_0^1 U^I_{\Delta x,\Delta t}(x,t_k)dx$, $I=1,2$ for Figure 7 and $Z_k=(1+\varepsilon_k)\sum_{I=1}^{2}\int_0^1 U^I_{\Delta x,\Delta t}(x,t_k)dx$ for Figure 8, where $\varepsilon_{I,k}$ and ε_k each are the random sample from a normal random number generator with mean zero and standard deviation $\sigma=0.02$.

We choose the parameter space $Q=\mathcal{D}\times\mathcal{D}$. Clearly, Q is compact in $\mathcal{C}[0,1]\times\mathcal{C}[0,1]$. We approximate the infinite-dimensional parameter space as follows: For M_1, M_2 positive integers and any $(b_1,b_2)\in Q$, we set

$$(\mathcal{I}_{M_J}b^J)(x)=\sum_{i=1}^{M_J-1} b^J\left(\frac{i}{M_J}\right)\phi^i_{M_J}(x;0,1),\quad J=1,2.$$

Clearly, $\lim_{M_J\to\infty}\mathcal{I}_{M_J}b^J=b^J$ in $\mathcal{C}[0,1]$, uniformly in b^J, $J=1,2$. Hence, if $b^J_{M_J}\in Q_{M_J}=I_{M_J}(Q)$ is given by

$$b^J_{M_J}(x)=\sum_{i=1}^{M_J-1}\lambda^{J,i}_{M_J}\phi^i_{M_J}(x;0,1),\quad J=1,2,$$

then the solution of our finite-dimensional identification problem involves identifying the M_1+M_2-2 coefficients $\{\lambda^{J,i}_{M_J}\}_{i=1,J=1}^{M_J-1,2}$ from a compact subset of $\mathbb{R}_+^{M_1+M_2-2}$ so as to minimize the least squares cost functional (9) or (10).

To indirectly implement the compactness constraints of Q, we still use the regularized least squares cost functional. For Figure 7, we use the form

$$\begin{aligned}\mathcal{J}_{\Delta x,\Delta t}(q) &= \sum_{I=1}^{2}\sum_{k=1}^{m}\left|\log\left(\int_0^1 U^I_{\Delta x,\Delta t}(x,t_k;q)dx+1\right)-\log(Z_{I,k}+1)\right|^2\\ &\quad+\sum_{I=1}^{2}\alpha_I\int_0^1\left|\frac{d}{dx}b^I_{M_I}(x)\right|^2dx,\end{aligned}$$

and for Figure 8, we use the form

$$\begin{aligned}\mathcal{J}_{\Delta x,\Delta t}(q) &= \sum_{k=1}^{m}\left|\log\left(\sum_{I=1}^{2}\int_0^1 U^I_{\Delta x,\Delta t}(x,t_k;q)dx+1\right)-\log(Z_k+1)\right|^2\\ &\quad+\sum_{I=1}^{2}\alpha_I\int_0^1\left|\frac{d}{dx}b^I_{M_I}(x)\right|^2dx,\end{aligned}$$

where $\alpha_I>0$, $I=1,2$ are the regularization parameters, and $m=100$ for Figures 7 and 8.

In the rest of our simulations, we use $\Delta x=\Delta t=0.005$ to generate the data and $\Delta x=\Delta t=0.01$ to solve the least squares. Thus, in these cases the data are not exactly attained by our model even if the noise is removed.

The upper-left part and the lower-left part of the following two figures represent the S (=1,000) numerical results of the estimated parameters $b^1_{M_1}(x)$ and $b^2_{M_2}(x)$ versus the exact parameters $b^1(x)$ and $b^2(x)$, respectively. The upper-right part and the lower right part represent the figures of the corresponding 95% confidence interval (dashed line) versus the exact $b^1(x)$ and $b^2(x)$ (solid line), respectively. The tables provide statistical results for the corresponding graphs.

Note that the results in Figure 7 and Table 7 are slightly better than those in Figure 8 and Table 8. This is expected since in Figure 7 we are sampling data for each of the two populations, which provides more information than sampling the sum of the two populations only, as is the case in Figure 8. Also note that in both of these figures we let $M = M_1 = M_2 = 10$.

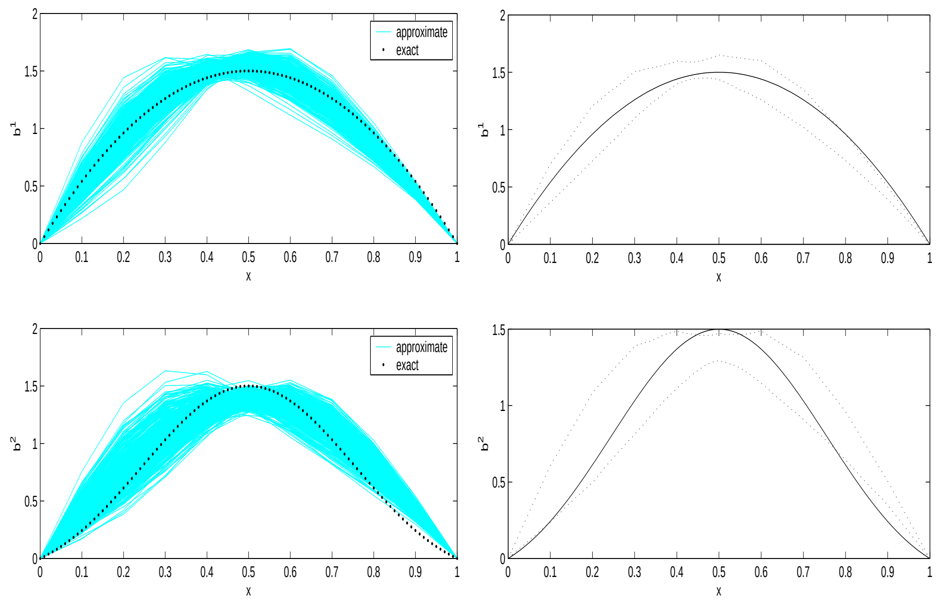

FIGURE 7. $M = 10$, $\alpha_1 = 5e-5$, $\alpha_2 = 5e-5$. Each of the grey lines (....) of the left part of the figure denotes a distinct result for a given sample $\{\epsilon_{I,k}\}$.

TABLE 7. Statistical results of $b^1(x)$ and $b^2(x)$ for Figure 7

$b^1(x)$				$b^2(x)$			
x	$AB(x)$	$RAB(x)$	$SE(x)$	x	$AB(x)$	$RAB(x)$	$SE(x)$
0.1	-0.0187	-3.4717	0.0880	0.1	0.1684	69.4034	0.0959
0.2	-0.0004	-0.0447	0.1276	0.2	0.1628	26.5887	0.1528
0.3	0.0334	2.6514	0.1053	0.3	0.0487	4.7244	0.1483
0.4	0.0562	3.9007	0.0493	0.4	-0.0728	-5.3114	0.0946
0.5	0.0449	2.9941	0.0548	0.5	-0.1134	-7.5604	0.0464
0.6	-0.0040	-0.2805	0.0860	0.6	-0.0437	-3.1871	0.0860
0.7	-0.0683	-5.4239	0.0836	0.7	0.0931	9.0282	0.1053
0.8	-0.1101	-11.4644	0.0576	0.8	0.2039	33.3052	0.0819
0.9	-0.0929	-17.2091	0.0272	0.9	0.1954	80.5164	0.0402

4. **Concluding remarks.** In this paper, we have developed a numerical technique for identifying unknown parameters in a general size-structured population model. A main focus of the paper is on a statistical study of the parameter-estimation technique. This was carried out by calculating pointwise standard errors on the

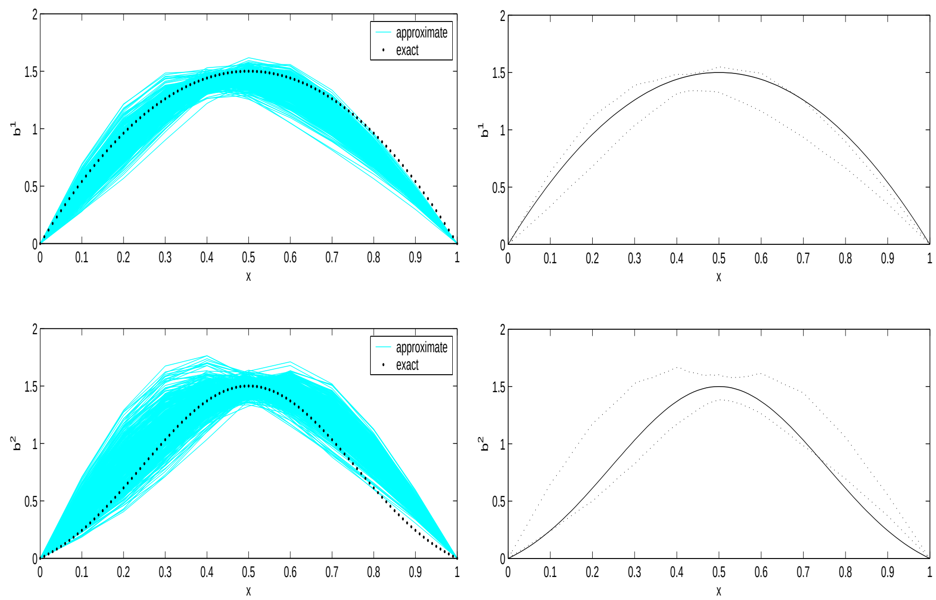

FIGURE 8. $M = 10$, $\alpha_1 = 5e-5$, $\alpha_2 = 5e-5$. Each of the grey lines (....) of the left part of the figure denotes a distinct result for a given sample $\{\epsilon_k\}$.

TABLE 8. Statistical results of $b^1(x)$ and $b^2(x)$ for Figure 8

$b^1(x)$				$b^2(x)$			
x	$AB(x)$	$RAB(x)$	$SE(x)$	x	$AB(x)$	$RAB(x)$	$SE(x)$
0.1	-0.0687	-12.7279	0.0765	0.1	0.1926	79.3867	0.1066
0.2	-0.0790	-8.2334	0.1096	0.2	0.2106	34.4018	0.1757
0.3	-0.0572	-4.5419	0.0891	0.3	0.1187	11.5041	0.1784
0.4	-0.0402	-2.7920	0.0435	0.4	0.0178	1.2960	0.1208
0.5	-0.0537	-3.5800	0.0588	0.5	-0.0069	-0.4598	0.0549
0.6	-0.0980	-6.8075	0.0871	0.6	0.0665	4.8565	0.0915
0.7	-0.1490	-11.8273	0.0846	0.7	0.1889	18.3112	0.1157
0.8	-0.1694	-17.6443	0.0596	0.8	0.2704	44.1765	0.0915
0.9	-0.1255	-23.2483	0.0296	0.9	0.2239	92.2680	0.0459

estimated parameters (functions) through the use of thousands of numerical experiments.

Several conclusions can be drawn from our studies:

1. The method discussed above seems to perform well and produce good confidence intervals for the parameters.
2. When the infinite-dimensional effects of the model and the parameter space are removed, the resulting numerical and statistical values suggest that the least squares technique produces very good unbiased parameter estimates.
3. The type of numerical scheme used for approximating the infinite-dimensional model as well as the parameter space may influence the bias in the parameter-estimation technique.

4. The commonly used regularization term is crucial for enforcing compactness and for obtaining better estimates. However, it may also introduce more bias in the estimator.

We note in closing that the system (1) investigated in this paper is a special case of the measure-dependent aggregate dynamics problems formulated in [6], wherein individual (uncoupled) dynamics are not available. Inverse problems for such systems have been investigated in a number of applications, including cellular level HIV modelling [7], hysteresis in viscoelastic materials [8, 9], shear waves in biotissue [10], and electromagnetic interrogation in complex materials [11]. In a more general formulation (currently under investigation by the authors), one has a probability distribution F of individual parameters $q(x,P) = q = (g,m,\beta,C)$ on an admissible set Q. The system (1) is replaced by a continuum of systems for $u(x,t;q(x,P))$ with the total population $P(t;F)$ given by

$$P(t;F) = \int_Q \left[\int_0^L u(x,t;q)dx\right] dF(q) = \int_Q \left[\int_0^L u(x,t;q)dx\right] f(q)dq;$$

the latter equality holds if F has a density f. The aggregate dynamics for u depend explicitly on F through the dependence of the individual rate parameters (g,m,β,C) on the total population P.

If F is a discrete measure with N atoms at q^J of mass f_J, then we have

$$P(t;F) = \sum_{J=1}^N f_J \int_0^L u(x,t;q^J)dx.$$

Moreover, if F is uniformly and discretely distributed ($f_J = \frac{1}{N}$), this becomes

$$P(t;F) = \frac{1}{N}\sum_{J=1}^N \int_0^L u(x,t;q^J)dx,$$

which is simply a scaled (by $\frac{1}{N}$) version of (2). Of course, even in this simple case, the system does not decouple (i.e., individual dynamics are not available). This will be the case any time the individual parameters for subpopulations depend on the total population. It is also clear that inverse problems with such measure-dependent dynamics are a generalized version of the estimation problems discussed in the statistical literature in the context of hierarchial or mixed effects modelling [20, 21, 22].

Acknowledgments. The work of A. S. Ackleh and S. Hu was supported in part by the National Science Foundation under grant no. DMS-0311969. The work of K. Deng was supported in part by the National Science Foundation under grant no. DMS-0211412. The work of H. T. Banks was supported in part by the US Air Force Scientific Research under grant no. AFOSR FA9550-04-1-0220 and in part by the Joint DMS/NIGMS Initiative to Support Research in the Area of Mathematical Biology under grant no. 1R01GM67299-01. The authors thank Professor N. Pal for extensive discussions concerning the statistical aspects of this work.

Collaboration was also facilitated by Ackleh's visits to the Statistical and Applied Mathematical Sciences Institute (SAMSI), Research Triangle Park, North Carolina, which was funded by the National Science Foundation under grant no. DMS-0112069.

REFERENCES

[1] A. S. Ackleh, Parameter estimation in the nonlinear size-structured population model, Advances in Systems Science and Applications, special issue (1997), 315–320.

[2] A. S. Ackleh, Estimation of parameters in a structured algal coagulation-fragmentation model, Nonlinear Anal. 28 (1997), 837–854.

[3] A. S. Ackleh, Parameter identification in size-structured population models with nonlinear individual rates, Math. Comput. Modelling 30 (1999), 81–92.

[4] A. S. Ackleh, H. T. Banks, and K. Deng, A finite difference approximation for a coupled system of nonlinear size-structured populations, Nonlinear Anal. 50 (2002), 727–748.

[5] B. M. Adams, H. T. Banks, J. E. Banks, and J. D. Stark, Population dynamics models in plant-insect herbivore-pesticide interactions, (Tech. Rep. No. CRSC-TR03-12), Center for Research in Scientific Computation, North Carolina State University, Raleigh, NC, 2003; Math. Biosci. (to appear).

[6] H. T. Banks, D. M. Bortz, G. A. Pinter, and L. K. Potter, Modeling and imaging techniques with potential for application in bioterroism, (Tech. Rep. No. CRSC-TR03-02), Center for Research in Scientific Computation, North Carolina State University, Raleigh, NC, 2003; chap. 6 in Bioterrorism: Mathematical Modeling Applications in Homeland Security, (ed. H. T. Banks and C. Castillo-Chavez), *Frontiers in Applied Math, FR28*, SIAM, Philadelphia, 2003, 129–154.

[7] H. T. Banks, D. M. Bortz, and S. E. Holte, Incorporation of variability into the modeling of viral delays in HIV infection dynamics, (Tech. Rep. No. CRSC-TR01-25), Center for Research in Scientific Computation, North Carolina State University, Raleigh, NC, 2001 (rev. Nov. 2001); Math. Biosci. 183 (2003), 63–91.

[8] H. T. Banks, N. G. Medhin, and G. A. Pinter, Multiscale considerations in modeling of nonlinear elastomers. (Tech. Rep. No. CRSC-TR03-42), Center for Research in Scientific Computation, North Carolina State University, Raleigh, NC, 2003; J. Comp. Math. Sci. and Engr. (to appear).

[9] H. T. Banks, N. G. Medhin, and G. A. Pinter, Nonlinear reptation in molecular based hysteresis models for polymers, (Tech. Rep. No. CRSC-TR03-45), Center for Research in Scientific Computation, North Carolina State University, Raleigh, NC, 2003; Quart. Appl. Math. 62 (2004), 767–779.

[10] H. T. Banks and G. A. Pinter, A probabilistic multiscale approach to hysteresis in shear wave propagation in biotissue, (Tech. Rep. No. CRSC-TR04-03), Center for Research in Scientific Computation, North Carolina State University, Raleigh, NC, 2004; SIAM J. Multiscale Modeling and Simulation (to appear).

[11] H. T. Banks and N. L. Gibson, Well-posedness in Maxwell systems with distributions of polarization relaxation parameters, (Tech. Rep. No. CRSC-TR04-01), Center for Research in Scientific Computation, North Carolina State University, Raleigh, NC, 2004; Applied Math. Letters 18 (2005), 423–430.

[12] H. T. Banks, Computational techniques for inverse problems in size-structured population models, Proc. IFIP Conf. on Optimal Control of Systems Governed by PDE (Santiago de Compostela, July 1987), Lecture Notes in Control and Info. Science, 114, Springer-Verlag, Berlin, 1988, 3–10.

[13] H. T. Banks, Some remarks on estimation for size-strucutred population models in *Frontiers of Theoretical Biology*, ed. S. Levin, Lecture Notes in Biomathematics, 100, Springer-Verlag, Berlin, 1994, 609–623.

[14] H. T. Banks, L. Botsford, F. Kappel, and C. Wang, Modeling and estimation in size structured population models, Mathematical Ecology (Proc. Trieste, 1986), World Sci., Singapore, 1988, 521–541.

[15] H. T. Banks, L. W. Botsford, F. Kappel, and C. Wang, Estimation of growth and survival in size-structured cohort data: An application to larval striped bass (Morone Saxatilis), J. Math. Biol. 30 (1991), 125–150.

[16] H. T. Banks and B. G. Fitzpatrick, Estimation of growth rate distributions in size structured population models, Quart. Appl. Math. 49 (1991), 215–235.

[17] H. T. Banks, B. G. Fitzpatrick, L.K. Potter, and Y. Zhang, Estimation of probablity distributions for individual parameters using aggregate popultion observations,

Stochastic Analysis, Control, Optimization and Applications, ed. W. Mceneney, G. Yin, Q. Zhang, Birkhäuser, Basal, 1998, 353–371.
[18] H. T. Banks and K. Kunisch, Estimation techniques for distributed parameter systems, Birkhauser, Boston, 1989.
[19] K. Cho and Y. Kwon, Parameter estimation in nonlinear age-dependent population dynamics, IMA J. Appl. Math. 62 (1999), 227–244.
[20] M. Davidian and A. R. Gallant, The nonlinear mixed effects model with a smooth random effects density, Biometrika 80 (1993), 475–488.
[21] M. Davidian and D. M. Giltinan, Nonlinear models for repeated measurement data, Chapman and Hall/CRC, New York, 1995.
[22] M. Davidian and D. M. Giltinan, Nonlinear models for repeated measurement data: An overview and update, J. Agricul. Biol and Environ. Statistics 8 (2003), 387–419.
[23] G. Di Cola and F. Nicoli, Parameter estimation in age-structured population dynamics, Riv. Mat. Univ. Parma. 9 (1983), 213–222.
[24] O. Diekmann, M. Gyllenberg, J. A. Metz, and H. Thieme, The "cumulative" formulation of (physiologically) structured population models, Evolution equations, control theory, and biomathematics (Proc. Han sur Lesse, 1991), Lecture Notes in Pure and Appl. Math. 155, Dekker, New York, 1994, 145–154.
[25] G. Dimitriu, Parameter estimation in size/age structured population models using the moving finite element method, Numerical methods and applications, Lecture Notes in Comput. Sci. 254, Springer-Verlag, Berlin, 2003, 420–429.
[26] H. W. Engl, W. Rundell, and O. Scherzer, A regularization scheme for an inverse problem in age-structured populations, J. Math. Anal. Appl. 182 (1994), 658–679.
[27] B. G. Fitzpatrick, Modeling and estimation problems for structured heterogeneous populations, J. Math. Anal. Appl. 172 (1993), 73–91.
[28] B. G. Fitzpatrick, Statistical tests of fit in estimation problems for structured population modeling, Quart. Appl. Math. 53 (1995), 105–128.
[29] M. Grasselli, An inverse problem in population dynamics, Numer. Funct. Anal. Optim. 18 (1997), 311–323.
[30] M. Gyllenberg, A. Osipov and L. Päivärinta, The inverse problem of linear age-structured population dynamics, J. Evol. Equ. 2 (2002), 223–239.
[31] P. Hall and D. M. Titterington, On confidence bands in nonparametric density estimation and regression, J. Multivariate Anal. 27 (1988), 228–254.
[32] W. Härdle, Asymptotic maximal deviation of M-smoothers, J. Multivariate Anal. 29 (1989), 163–169.
[33] V. Hutson and J. S. Pym, Applications of functional analysis and operator theory, Academic Press, New York, 1980.
[34] W. Huyer, A size stuctured population model with dispersion, J. Math. Anal. Appl. 181 (1994), 716–754.
[35] B. G. Lindsay, The geometry of mixture likelihoods: I and II, Annal. Statist. 11 (1983), 86–94, and 783–792.
[36] A. Mallet, A maximum-likelihood estimation method for random coefficient regression models, Biometrika 73 (1986), 645–656.
[37] F. A. Milner and G. Rabbiolo, Rapidly converging numerical algorithms for models of population dynamics, SIAM J. Numer. Anal. 30 (1993), 733–753.
[38] D. Nychka, Bayesian confidence intervals for smoothing splines, J. Amer. Statist. Assoc. 83 (1988), 1134–1143.
[39] D. Nychka, The average posterior variance of a smoothing spline and a consistent estimate of the average squared error, Annal. Statist. 18 (1990), 415–428.
[40] M. S. Pilant and W. Rundell, Determing a coefficient in a first-order hyperbolic equation, SIAM J. Appl. Math. 51 (1991), 494–506.
[41] J. Ripoll, J. Saldaña, and J. C. Senar, Evolutionarily stable transition rates in a stage-structured model. An application to the analysis of size distributions of badges of social status, Math. Biosci. 190 (2004), 145–181.
[42] W. Rundell, Determing the birth function for an age-structured population, Math. Population Stud. 1 (1989), 377–395.
[43] W. Rundell, Determing the death rate for an age-structured population from census data, SIAM J. Appl. Math. 53 (1993), 1731–1746.
[44] M. H. Schultz, Spline analysis, Prentice-Hall, Englewood Cliffs, New Jersy, 1973.

[45] A. Sen and M. Srivastava, Regression analysis: theory, methods and applications, Springer-Verlag, New York, 1990.

[46] A. van der Vaart, Efficient maximum likelihood estimation in semiparametric mixture models, Annal. Statist. 24 (1996), 862–878.

[47] N. M. Van Straalen, The "inverse problem" in demographic analysis of stage-structured populations, The dynamics of physiologically structured populations (Amsterdam, 1983), Lecture Notes in Biomathematics 68, Springer-Verlag, Berlin, 1986, 393–408.

[48] G. Wahba, Bayesian confidence intervals for the cross-validated smoothing splines, J. R. Statist. Soc. B. 45 (1983), 133–150.

[49] S. N. Wood and R. M. Nisbet, Estimation of mortality rates in stage-structured population, Lecture Notes in Biomathematics 90, Springer-Verlag, Berlin, 1991.

Received on May 28, 2004. Revised on March 15, 2005.

E-mail address: ackleh@louisiana.edu
E-mail address: htbanks@unity.ncsu.edu
E-mail address: deng@louisiana.edu
E-mail address: sxh5554@louisiana.edu